Contents lists available at ScienceDirect

# Science of the Total Environment

Research Paper

# Use of iron-coated sand for removing soluble phosphorus from drainage water

Wim J. Chardon [a,1], Jan E. Groenenberg [b], Jos P.M. Vink [c], Andreas Voegelin [d], Gerwin F. Koopmans [b,*]

[a] Wageningen Environmental Research, Wageningen University and Research, P.O. Box 47, 6700 AA Wageningen, the Netherlands
[b] Chair Group Soil Chemistry and Chemical Soil Quality, Wageningen University and Research, P.O. Box 47, 6700 AA Wageningen, the Netherlands
[c] Deltares, Unit Subsurface & Groundwater Systems, P.O. Box 85467, 3508 AL Utrecht, the Netherlands
[d] Eawag, Swiss Federal Institute of Aquatic Science & Technology, CH-8600 Duebendorf, Switzerland

## HIGHLIGHTS

- P removal from drainage water by a pipe drain enveloped with Fe-coated sand was 93%.
- Fe in the sand particle coatings was mainly present as siliceous ferrihydrite (Fh).
- Reductive release of Fe(II) caused a gradual increase in effluent Fe over time.
- Fe loss was insignificant compared to the amount of Fe wrapped around the drain.
- Fh stability and its ability to retain P were not affected over time.

## GRAPHICAL ABSTRACT



Sand coated with siliceous ferrihydrite wrapped around pipe drain
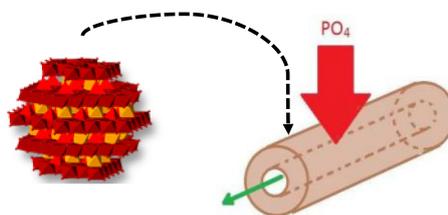
PO$_4$ removal from drainage water

## ARTICLE INFO

## ABSTRACT

Mitigation measures are needed for reducing chronic dissolved phosphorus (P) losses from agricultural soils with a legacy of excessive P inputs to surface waters. Since pipe drains are an important pathway for P transport from agricultural soils to surface waters in flat areas, removing P from drainage water can be an effective measure. During a 4.5 year-field experiment, we tested the performance of a pipe drain enveloped with Fe-coated sand for removing soluble P from drainage water. Iron-coated sand is a by-product of the drinking water industry and has a high ability to bind P. The P concentration in the effluent from the enveloped pipe drain remained at a very low level over the entire monitoring period, with a removal percentage amounting to 93% for total P. During the field experiment, the enveloped pipe drain was below the groundwater level for a prolonged time. Nevertheless, no reduction of Fe(III) in the Fe-coated sand occurred during the first two years, most likely due to preferential reduction of Mn oxides present in the coatings of the sand particles, as reflected in elevated effluent Mn concentrations. Thereafter, reductive dissolution of Fe oxides in the coatings caused a gradual increase in the Fe concentration in the enveloped pipe drain effluent over time. Concomitantly, the dissolved Mn concentration decreased, most probably due to the depletion in easily accessible Mn oxides in the Fe-coated sand. The Fe in the Fe-coated sand was identified as silicate-containing ferrihydrite (Fh). The submerged conditions of the enveloped pipe drain neither affected the stability of Fh in the Fe-coated sand nor the ability of this measure to capture P from drainage water. Enveloping pipe drains with Fe-coated sand is an effective method for reducing dissolved P inputs from agricultural soils to surface waters and holds great promise for implementation in practice.

---

* Corresponding author.
   E-mail address: gerwin.koopmans@wur.nl (G.F. Koopmans).
[1] [retired].

## 1. Introduction

Surface water eutrophication, and dense blooms of cyanobacteria in surface waters as a possible consequence, are problems water managers are still facing worldwide (Stroom and Kardinaal, 2016). While point sources of phosphorus (P) have often been reduced effectively, diffuse sources still remain (Macintosh et al., 2018). Due to over-fertilization in the past, many soils became saturated with P and a large part of their adsorption capacity is now filled with P (Schoumans and Chardon, 2015; Kleinman, 2017). Soil P reserves from historic P applications, also called legacy P (Sharpley et al., 2013), may reduce the effectiveness of source-oriented measures taken for preventing dissolved P losses from agricultural land to surface waters. For example, depleting a soil by crop removal without replacing P taken up by the crop (phytomining) can be an effective option for reducing the risk of P leaching (Koopmans et al., 2004; van der Salm et al., 2009; Kleinman et al., 2011). However, when the size of the soil legacy P pool is large, the short-term effect of phytomining on surface water quality can be small (McCrackin et al., 2018). Therefore, other options are needed, since a fast improvement of water quality is often necessary. For example, the water quality standards of the European Water Framework Directive (EC 2000/60/EC) will have to be met ultimately in 2027. One option to realize this can be the use of reactive materials for binding P, either for immobilizing P in the topsoil (Koopmans et al., 2020) or for retaining P in buffer strips, vertical barriers, and filter systems (Klimeski et al., 2012; Groenenberg et al., 2013). These reactive materials often contain Fe or Al oxides (Cucarella and Renman, 2009), which are characterized by a large specific surface area and a high P adsorption site density (Celi et al., 2003; Hiemstra, 2018; Hiemstra et al., 2019; Hiemstra and Zhao, 2016; Koopmans et al., 2020; Wang et al., 2013). In flat areas, drainage can be more important for discharging excess water from agricultural land than surface runoff-mediated transport (King et al., 2015). In such areas, artificial pipe drainage is usually installed for maintaining a low groundwater level. In The Netherlands, 40% of the agricultural land is drained by pipe drains (Groenenberg et al., 2013). Reactive materials can then be applied around the pipe drains (McDowell et al., 2008; Groenenberg et al., 2013), or in filters at the end of the pipe drains (Buda et al., 2012; Canga et al., 2016a, 2016b; Penn et al., 2014, 2017; Vandermoere et al., 2018). Groenenberg et al. (2013) described a field experiment with a pipe drain enveloped with sand, coated with Fe oxides (further denoted as Fe-coated sand), which is a by-product of the production of drinking water from anoxic groundwater (Sharma et al., 2002; van Beek, 2018). Sharma et al. (2002) characterized Fe-coated sand from 12 drinking water production plants in The Netherlands, where anoxic groundwater is led over a sand filter in order to remove dissolved Fe(II) by aeration of the raw water. In the coating of the sand particles from these drinking water production locations, they observed amorphous Fe oxides in combination with Ca, silicate, and Mn oxides. Aeration of Fe(II)-containing water in the presence of silicate can lead to the formation of siliceous ferrihydrite (Fh) at which the adsorption of silicate suppresses the growth of Fh particles (Hiemstra, 2018; Kaegi et al., 2010; Koopmans et al., 2020; Voegelin et al., 2010) while at the same time these particles can densely aggregate under the influence of Ca (Kaegi et al., 2010; Voegelin et al., 2010). The enveloped pipe drain in the field experiment of Groenenberg et al. (2013) was installed on a site with a calcareous sandy soil located in a seepage polder (Griffioen, 1994) on which flower bulbs were grown and where concentrations of dissolved reactive phosphorus (DRP) in the water from pipe drains were excessive (2—4 mg L$^{-1}$). This can at least partly be ascribed to high concentrations of DRP in seepage water at this location and a net P surplus of 18 kg P ha$^{-1}$ yr$^{-1}$ due to compost addition (Groenenberg et al., 2013) in combination with the generally low P binding capacity of calcareous sandy soils (Chardon and Schoumans, 2007; Koopmans et al., 2006; Schoumans, 2014). The results from the first 15 months of this field experiment were reported by Groenenberg et al. (2013). The main conclusions were: (i) the enveloped pipe drain was very effective in capturing DRP from drainage water, with an average DRP reduction of 94% and (ii) reductive dissolution of Mn oxides present in the

Fe-coated sand prevented the reductive release of Fe(II) from Fe(III) oxides in the Fe-coated sand under submerged conditions. However, the results of Groenenberg et al. (2013) do not provide insight in the ability of the enveloped pipe drain to retain P from drainage water on the longer term. Consequently, it is difficult to assess whether this measure can be implemented in practice. Important research gaps which need further experimental research include the effect of submerged conditions on reductive dissolution of Mn oxides in the Fe-coated sand and how this affects the stability of Fe(III) oxides and their ability to capture P from drainage water on the long term. In the experimental approach of Groenenberg et al. (2013), soil pore water samples were taken in-situ from suction cups either above, 10 cm beside, or 15 cm below the envelope with Fe-coated sand. The chemical composition of these pore water samples indicated anoxic conditions below and beside the enveloped pipe drain. However, this experimental approach did not allow for the determination of the effect of submerged conditions on the stability of Fe(III) oxides and P binding inside the envelope with Fe-coated sand. In our current study, a SOFIE® cell (*Sediment Or Fauna Incubation Experiment tool*; Vink, 2002, 2009) was used to collect an undisturbed core sample from the envelope of the pipe drain in-situ to enable direct pore water sampling and measurements in the laboratory while preserving redox-discrete field conditions in the core sample. Also, in-situ transformation of the Fe oxides in the sand coatings over time into more crystalline Fe phases is an important issue, as this can affect the ability of the enveloped pipe drain to retain P from drainage water. For example, Nielsen et al. (2014) found a half-life of 4 years for the transformation of a siliceous Fh, formed by aerating anoxic groundwater, into goethite after burying it into soil. The maximum P adsorption density for goethite is limited to about 2.5 to 3.5 µmol m$^{-2}$ (Hiemstra and van Riemsdijk, 1996) whereas the maximum P adsorption density of Fh is usually higher (Celi et al., 2003; Hiemstra and Zhao, 2016; Koopmans et al., 2020; Wang et al., 2013). The aims of our current study are (i) to quantify P retention by the enveloped pipe drain for an extended period of time, i.e., a monitoring period with a total duration of 54 months instead of the first 15 months for which data has been reported by Groenenberg et al. (2013), (ii) to test if continuing Mn release from reduction of Mn oxides still prevented reductive dissolution of Fe oxides, (iii) to quantify the effects of (an)oxic conditions on the stability of Fe(III) oxides and P binding inside an undisturbed Fe-coated sand core sampled by using a SOFIE® cell, and (iv) to characterize the Fe oxides in the envelope with Fe-coated sand using X-ray absorption spectroscopy (XAS). Results of this extended field experiment will help to support the evaluation of the long-term effectiveness of enveloping pipe drains with Fe-coated sand to prevent P loss to surface waters for implementation in practice.

## 2. Materials and methods

### 2.1. Site description and field experiment

The experiment was done on a field used for flower bulb growth, on a calcareous sandy soil in a seepage polder in the Dutch coastal area (Griffioen, 1994) near Egmond aan den Hoef. The field site has a net P surplus since more P is applied via compost than is removed with harvesting, leading to a build-up of P in the soil profile and leaching of P. The experimental setup of the field experiment was extensively described in Groenenberg et al. (2013). In brief, the enveloped pipe drain was installed between two existing pipe drains, which were used as a reference in this field experiment. For the installation of the enveloped pipe drain, a 55 m-long trench was dug (depth 90 cm and width 40 cm). In the trench, a coconut fiber cloth was placed, then a 10-cm layer of Fe-coated sand with a new 6-cm-i.d. polyvinyl chloride pipe drain placed on the sand. The trench was filled beside the pipe drain with Fe-coated sand and a 10- to 20-cm layer of coated sand was placed on top of the drain. The coconut cloth was folded and the trench was filled with original soil. A total of 0.14 m$^3$ of Fe-coated sand was estimated to be used per m drain, containing 65 kg Fe per m drain (see Section S1 in the Supplementary data).

Water samples from the outlet of the enveloped pipe drain and the two reference drains were collected during the winter periods (October to March), when rainfall usually exceeds evaporation in The Netherlands. The outlet of the pipe drains was below the water level of the ditch most of the time, as common in this region. Only when water turbulence in the ditch at the drain outlet indicated water discharge from a drain, the effluent was sampled. To avoid sampling inflowing ditch water, effluent water samples were taken via a 2-m-long tube, inserted into the pipe drains via the outlet. During the experimental period October 2010 to April 2015 (54 months), water samples were taken at 32 sampling events from the pipe drain outlets. At all sampling events, also a water sample from the receiving ditch was taken close to the reference pipe drains.

For sampling the soil pore water around the enveloped pipe drain, polyester acrylate suction cups were installed along the enveloped drain at 5, 15, 25, and 45 m from the ditch. The permeability of these cups is around 0.1 μm (Groenenberg et al., 2013). At each position, one cup was installed 15 cm below, two cups at 10 cm on either side, and one cup straight above the envelope with Fe-coated sand. Soil pore water samples were collected via vacuum bottles (approximately 90 kPa), connected to the cups. Before analysis, the pore water samples from all cups placed at the same height were combined for making a composite sample. From January 2011 to July 2014 (42 months), a total of 23 soil pore water samples were obtained for the suction cups placed above or below the enveloped pipe drain. For the cups placed beside the enveloped pipe drain, no pore water samples could be taken at two sampling events. For these cups, the composite pore water samples of 21 sampling events were analysed.

### 2.2. Chemical water analyses

Directly after sampling, water samples from the pipe drains and ditch were split in-situ into a filtered (0.45 μm) and an unfiltered portion. During the first 10 months of the field experiment (13 sampling events), the pH was measured in-situ in the composite water samples from the suction cups using a HI 9828 Multiparameter Water Quality Portable Meter (Hanna Instruments). All water samples were transported immediately to the laboratory in a cool box and stored at 5 °C until analysis within 1 week of sampling. In the composite water samples from the suction cups and in the 0.45 μm-filtered samples from the pipe drains and ditch, ortho-P was measured as DRP according to Murphy and Riley (1962) using a segmented flow analyzer (SFA; Skalar, SK12) (Houba et al., 2000). Concentrations of metals (Ca, Fe, and Mn), total dissolved P (TDP), and S were measured using an inductively coupled plasma–atomic emission spectrometer (ICP–AES; Iris-3300 DV, Thermo), after acidification to pH 1. Chloride was measured using a flow injection analyzer (FIA). Dissolved unreactive P (DUP) was calculated as the difference between TDP and DRP. Concentrations of $NH_4$–N, $(NO_3 + NO_2)$-N, and total dissolved N (TDN) in the composite water samples from the suction cups were measured using the SFA (Houba et al., 2000). Dissolved organic N (DON) was calculated as the difference between TDN and the summed $NH_4$–N and $(NO_3 + NO_2)$-N concentrations. Before the SFA analyses of DRP and the different N forms, the samples were acidified by HCl addition to lower the pH to approximately 2 to dissolve Fe(III)-containing colloids which could have been formed in anaerobic water samples due to exposure to air during transport and storage. Dissolved organic C (DOC) in the composite water samples from the suction cups was measured with a Total Organic Carbon analyzer (TC5000, Shimadzu) and calculated as the difference between total and inorganic C. In the unfiltered part of the pipe drain effluent and ditch water samples, total P was measured after peroxidation digestion ($H_2SO_4$, $H_2O_2$, and Se). Particulate P (PP) was calculated as the difference between TP and TDP. For further analytical details, see Groenenberg et al. (2013).

### 2.3. Sampling of Fe-coated sand from the enveloped pipe drain

Before applying Fe-coated sand for enveloping the pipe drain, a grab sample was taken from the Fe-coated sand in the field (denoted as $t_0$) and

field sampling was done after 14, 32, and 59 months (denoted as $t_{14}$, $t_{32}$, and $t_{59}$), each time on a new location along the drain. The last sampling of Fe-coated sand at $t_{59}$ fell outside the period of 54 months when the pipe drain effluent was monitored. For the field sampling of the Fe-coated sand from the envelope of the pipe drain, soil (circa 60 cm) above the drain was removed (Groenenberg et al., 2013). Using a piston sampler of 30 cm length, a sample was taken from the entire Fe-coated sand layer. The sample was divided in the field in portions originating either from below, beside, or above the enveloped pipe drain, further denoted as the lower layer (L), the middle layer (M), and the upper layer (U). This was done because the Fe-coated sand in the envelope is exposed to different redox conditions at various depths, as concluded from the measurements of the chemical soil pore water composition at different depths near the enveloped pipe drain (Groenenberg et al., 2013). After arrival in the laboratory, samples taken at $t_0$ and $t_{14}$ were air-dried at ambient temperature while samples taken at $t_{32}$ and $t_{59}$ were freeze-dried, both to avoid the risk of phase transformation of the Fe oxides during drying at elevated temperature (Schwertmann and Cornell, 1991; Chardon et al., 2012). At $t_{32}$, also an undisturbed Fe-coated sand core was collected in-situ with a SOFIE® cell (Vink, 2002, 2009) while preserving redox-discrete field conditions when the cell was transported to the laboratory. With this core, the entire Fe-coated sand layer of the enveloped pipe drain was sampled, with material from below, beside, and above the drain. The cell consists of a coring tube which is closed air-tight at both ends during sampling. Both pH and redox potential (Eh) were measured directly in the SOFIE® cell and via 0.1 μm-permeable probes the pore water in the core was sampled at the top, in the middle, and near the bottom of the intact core. Pore water samples were analysed on Cl, Br, F, $NO_3$-N, $NH_4$-N, $SO_4$-S, DRP, TDP, Fe, Mn, Na, and Ca. For details on the analytical techniques used for these chemical analyses, see Section S2 in the Supplementary data.

### 2.4. Pore water composition of Fe-coated sand

To quantify the chemical pore water composition inside the layer of Fe-coated sand enveloping the pipe drain, samples from the Fe-coated sand taken at $t_{32}$ and $t_{59}$ were extracted using 0.01 $M$ $CaCl_2$ at a solution-to-solid ratio (SSR) of 10 L $kg^{-1}$ (Houba et al., 2000). By shaking during extraction, Fe oxide colloids could be released from the coating of the sand particles, which can pass a 0.45 μm-filter. Therefore, the 0.01 $M$ $CaCl_2$ extraction method of Houba et al. (2000) was modified: shaking was done mildly at 30 rpm whereas the regular shaking time of 2 h was extended to 24 h to compensate for the mild shaking conditions. After 0.45 μm-filtration, the extracts were analysed on pH, Al, Fe, Mg, Mn, TDP, DRP, S, Si, DOC, As, Cd, Cu, Ni, Pb, and Zn, using the same analytical methods as described above in Section 2.2.

### 2.5. Total and acid ammonium oxalate-extractable element contents of Fe-coated sand

The Fe-coated sand samples taken at $t_0$, $t_{14}$, $t_{32}$, and $t_{59}$ were ground (50 μm) and subsequently digested with Aqua Regia (Houba et al., 1997) to determine the so-called "pseudo-total" contents of Fe, Al, Mn, and P (Quevauviller, 1998) in the material. For the Aqua Regia digestion, 0.5 g ground material was extracted with a 3:1 (v:v)-mixture of concentrated HCl and $HNO_3$. Furthermore, unground Fe-coated sand samples taken at $t_{32}$ and $t_{59}$ were extracted with 0.2 $M$ acid ammonium oxalate (Schwertmann, 1964; McKeague and Day, 1966) to determine the contents of amorphous Fe, Al, and Mn oxides and the content of reversibly adsorbed P. The Fe, Al, Mn, and P concentrations in the Aqua Regia digests and in the acid ammonium oxalate extracts (further denoted as $Fe_{ox}$, $Al_{ox}$, $Mn_{ox}$, and $P_{ox}$) were determined with ICP-AES. During acid ammonium oxalate extraction of soil, an SSR of 20 L $kg^{-1}$ and an extraction time of 2 h are often used (Schoumans, 2000). However, these extraction conditions are not sufficient to extract all amorphous Fe oxides and reversibly adsorbed P from this Fe-rich material (see Section S3 in the Supplementary data). For characterization of the Fe-coated sand, 1.5 g unground material was

extracted with 300 mL acid ammonium oxalate to realize an SSR of 200 L kg$^{-1}$ and the extraction time was extended to 4 h. The combination of an SSR of 200 L kg$^{-1}$ and 4 h was shown by Koopmans et al. (2020) to be sufficient for a complete extraction of both Fe$_{ox}$ and P$_{ox}$ from iron oxide sludge, which has even a higher Fe$_{ox}$ content than our Fe-coated sand (Chardon et al., 2012).

*2.6. Structural characterization of Fe in Fe-coated sand by X-ray absorption spectroscopy*

Four Fe-coated sand samples were characterized by Fe K-edge X-ray absorption spectroscopy (XAS): the grab sample collected at t$_0$ and samples taken at t$_{32}$ from different layers of the Fe-coated sand envelope. The samples taken at t$_{32}$ were frozen immediately after sampling in the field using liquid N$_2$ for preserving redox-discrete field conditions. The samples were ground in a mixer mill and mixed with cellulose for the preparation of a sample pellet. X-ray absorption spectra were recorded at the Swiss-Norwegian Beamline (SNBL) at the European Synchrotron Radiation Facility (ESRF, Grenoble). The measurements were performed in transmission mode at room temperature, using ionization chambers to record the incoming and transmitted X-ray photon intensity. For the extraction and interpretation of the extended X-ray absorption fine structure (EXAFS) spectra, the software code Athena was used (Ravel and Newville, 2005). For the interpretation of the spectra by linear combination fitting, we used four reference spectra: (i) lepidocrocite (Lp), (ii) goethite (Goe), and (iii) 2-line ferrihydrite (2L-Fh) formed by base addition to a concentrated Fe(NO$_3$)$_3$ solution (Voegelin et al., 2007) and (iv) silicate-containing Fh (Si-Fh) formed by the oxidation of 0.5 mM Fe(II) in a bicarbonate-buffered solution in the presence of 0.5 mM silicic acid (Senn et al., 2015). Owing to its formation in the presence of Si, Si-Fh features a lower degree of distortion of FeO$_6$ octahedra and of corner-sharing linkage of FeO$_6$ octahedra than 2L-Fh (Senn et al., 2015).

**3. Results and discussion**

*3.1. Chemical composition of soil pore water samples*

During a large part of the field experiment, suction cups directly above, beside, and 15 cm below the enveloped pipe drain were sampled. In Table 1, values of pH and the concentrations of major elements, several N species, and P fractions averaged over time are presented. The pattern obtained during the first 15 months (Groenenberg et al., 2013) was confirmed by the data for the whole experimental period. The soil pore water has a slightly alkaline pH and comparable Ca concentrations at all depths. For other elements, however, the concentrations in the soil pore water samples taken from the cups above the enveloped pipe drain differ strongly from those in the water from the cups below the drain. Above the enveloped pipe drain, the soil pore water is oxic, with 97% of the inorganic N being present as (NO$_3$ + NO$_2$)-N, with relatively low concentrations of Fe and Mn, and a high S concentration compared to the water from the cups below the drain. In contrast, the soil pore water from the cups below the drain is anoxic, with relatively high concentrations of Fe and Mn, a low S concentration, and inorganic N only being present as NH$_4$-N. These observations agree very well with the theoretical concept of redox-sensitive



**Fig. 1.** Dissolved reactive P (DRP) concentrations in the 0.45 μm-filtered water samples from the reference pipe drains and the enveloped pipe drain and the receiving ditch as a function of time (32 sampling events over 54 months of the whole field experiment).

chemical speciation of these elements at the transition from oxic to anoxic soil conditions (Kirk, 2004). On average, at all depths, DRP accounts for more than 90% of the TDP concentration over the entire period.

There is no indication that the composition of the water from the suction cup below the drain is influenced by the Fe-coated sand nearby. The high concentrations of Cl, Fe, Mn, DOC, NH$_4$, and P are indicative for brackish seepage water, as can be expected in a coastal area with peat layers in the subsoil (Griffioen, 1994). Increased DOC concentrations may well be explained by the mechanisms described by Vink et al. (2010): reductive production of Mn$^{2+}$ increases the metabolic fermentation of organic matter and the production of DOC, which subsequently prolongs the retention of metals and P in solution. Based on the Cl and S concentrations measured in the soil pore water from the cups at the three depths during the first sampling period, Groenenberg et al. (2013) concluded that downward drainage and upward seepage fluxes contributed equally to the water influx of the enveloped pipe drain. Data in Table 1 show that this remains more or less valid during the whole experiment, since the Cl and S concentrations in the soil pore water samples from the cups placed beside the enveloped pipe drain were close to the average of concentrations in the water from the cups above and below the drain.

*3.2. Leaching of P from the enveloped and reference pipe drains*

Fig. 1 shows the trend of the DRP concentration measured in the water samples from the ditch and the effluents of the reference pipe drains and enveloped pipe drain for the entire duration of the field experiment. Both reference pipe drains show a large temporal variation. Until the end of the experiment, the DRP concentrations measured in the effluent from the

**Table 1**
Concentrations of major elements, including inorganic C (IC), dissolved organic C (DOC), inorganic N, dissolved organic N (DON), dissolved unreactive P (DUP), and dissolved reactive P (DRP) in composite soil pore water samples from suction cups above, beside, and below the enveloped pipe drain averaged across the different sampling events ($n$ = 23) of the whole field experiment (54 months). Values represent average ± standard deviation.

| Position | pH[1] | Cl | Ca | Fe | Mn | S | IC | DOC | NH$_4$–N | (NO$_3$ + NO$_2$)-N | DON | DUP | DRP |
|---|---|---|---|---|---|---|---|---|---|---|---|---|---|
| | | mg L$^{-1}$ | | | | | | | | | | | |
| Above | 7.6 ± 0.3 | 28 ± 11 | 167 ± 41 | 1.2 ± 1.8 | 0.2 ± 0.3 | 78 ± 40 | 63 ± 16 | 26 ± 11 | 0.19 ± 0.24 | 6.91 ± 9.60 | 1.07 ± 0.37 | 0.05 ± 0.09 | 0.91 ± 1.16 |
| Beside | 7.5 ± 0.2 | 75 ± 31 | 154 ± 30 | 7.6 ± 3.0 | 0.7 ± 0.2 | 44 ± 25 | 96 ± 29 | 31 ± 12 | 1.75 ± 0.84 | 0.46 ± 0.66 | 1.45 ± 0.41 | 0.19 ± 0.47 | 2.49 ± 1.60 |
| Below | 7.4 ± 0.3 | 143 ± 37 | 179 ± 22 | 31.1 ± 10.4 | 3.4 ± 0.4 | 5.5 ± 6.3 | 154 ± 46 | 67 ± 46 | 8.12 ± 1.43 | 0.02 ± 0.05 | 2.52 ± 0.59 | 0.28 ± 0.82 | 3.48 ± 1.30 |

[1] pH of pore water in suction cups was measured in the field only during the first 10 months of the experiment (13 sampling events).
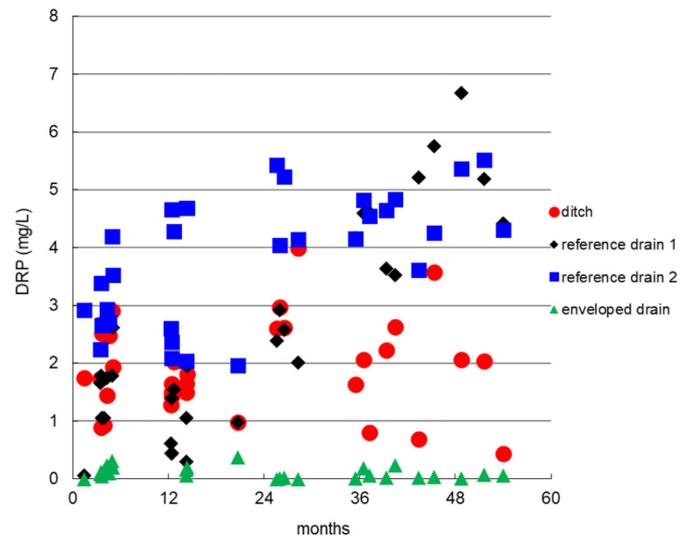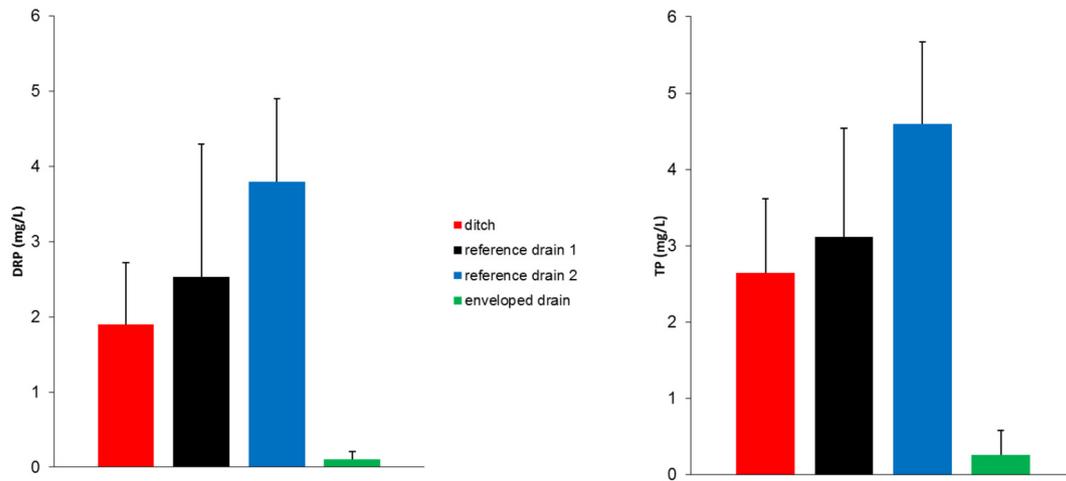
**Fig. 2.** Dissolved reactive P (DRP) in 0.45 μm-filtered water samples (left) and total P (TP) measured after peroxidation digestion of unfiltered water samples (right) from the receiving ditch, the reference pipe drains, and the enveloped pipe drain. Values represent average ± standard deviation over 54 months of the whole field experiment ($n = 32$).

enveloped pipe drain were clearly lower (factor of circa 30) than those for the reference pipe drains.

Overall, the average DRP concentration was 2.5 mg L$^{-1}$ for the reference pipe drain 1 and 3.8 mg L$^{-1}$ for the reference pipe drain 2 (Fig. 2). For the receiving ditch, an average value of 1.9 mg DRP L$^{-1}$ was found (Fig. 2). All values were higher than the average DRP concentrations reported by Groenenberg et al. (2013) for the first 15 months (reference pipe drain 1: 1.4 mg L$^{-1}$, reference pipe drain 2: 3.1 mg L$^{-1}$, receiving ditch: 1.7 mg L$^{-1}$).

For the enveloped pipe drain, an average DRP concentration of 0.10 mg L$^{-1}$ was found, much lower than the average DRP concentration of 3.16 mg L$^{-1}$ for the two reference pipe drains (Table 2). From these data, a removal percentage of 97% was calculated for DRP. Likewise, the DUP and PP concentrations are lower in the effluent from the enveloped pipe drain than for the reference pipe drains, but the removal percentage of both P forms is lower (81%) than for DRP. However, since the DRP fraction of TP exceeds 80% for the reference pipe drains, the removal percentage of TP is also high: 93% (Table 2). Hence, the enveloped pipe drain is very effective for retaining all these physical-chemical P fractions (Haygarth and Sharpley, 2000). Even after 54 months (4.5 year) of functioning, there is no indication of a decrease in the ability of the enveloped pipe drain to capture P from drainage water. Due to the lower removal percentage, the effluent from the enveloped pipe drain is relatively enriched with P fractions other than DRP: expressed as % of TP, the relative DUP and PP concentrations in the effluent of the enveloped pipe drain are about three times higher than in the effluent of the reference pipe drains (Table 2). However, the concentration of Fe in the enveloped pipe drain effluent is high when compared to TP (Table 2). The Fe, measured in the 0.45 μm-filtered water samples from this drain, will be present as either

dissolved Fe(II) or in colloidal particles. Baken et al. (2015) found that Fe (II), present in anoxic seepage water, was oxidized when the seepage water entered oxic layers of ditch sediments or in the overlying ditch water. The Fe(III) formed was able to immobilize DRP present in the ditch (Baken et al., 2015). Thus, the bioavailability of the P forms in the Fe-enriched enveloped pipe drain effluent and in the ditch water is probably low (Baken et al., 2014).

### 3.3. Leaching of Fe and Mn from the enveloped and reference pipe drains

Fig. 3 shows the average level of dissolved Fe in the 0.45 μm-filtered effluents of the reference pipe drains and the enveloped pipe drain and in the receiving ditch water for the duration of the whole experiment (54 months). Interestingly, the average Fe concentration during the first 15 months of the field experiment as reported by Groenenberg et al. (2013) completely differs from the period thereafter: during this first period, the average Fe concentration in the effluent from the enveloped pipe drain was much lower than in the effluents from the two reference pipe drains. This is remarkable, since soil pore water with a similarly high Fe concentration was probably transported with upward seepage from the subsoil to all pipe drains (see data from suction cup positioned below the enveloped pipe drain in Table 1). According to Fig. 4, the Fe concentration in the effluent from the enveloped pipe drain gradually increased over time to values around 33 mg L$^{-1}$ at the end of the experiment, which is much higher than the average values found in the effluents from the two reference pipe drains (Fig. 3). Although the Fe concentrations in the effluent from the enveloped pipe drain seem very high, they hardly exceed the average Fe concentration in the soil pore water, sampled via the suction cups placed 15 cm below the enveloped drain, i.e., 31.1 mg L$^{-1}$ (Table 1). Dilution of the high Fe

**Table 2**

Concentrations of different physical-chemical P fractions (DRP, DUP, PP, and TP) and Fe and Mn in effluent water samples from the enveloped pipe drain and from both reference pipe drains. Average values were calculated over the experimental period of 54 months ($n = 32$). Values represent average ± standard deviation.

| Drain | DRP | % sum[1] | DUP[2] | % sum[1] | PP[2] | % sum[1] | TP | Fe | Mn |
|---|---|---|---|---|---|---|---|---|---|
| | mg L$^{-1}$ | % | mg L$^{-1}$ | % | mg L$^{-1}$ | % | mg L$^{-1}$ | mg L$^{-1}$ | mg L$^{-1}$ |
| Reference[3] | 3.16 ± 1.60 | 80 | 0.16 ± 0.16 | 4 | 0.62 ± 1.01 | 16 | 3.86 ± 1.45 | 2.75 ± 1.71 | 1.01 ± 0.43 |
| With envelope | 0.10 ± 0.10 | 40 | 0.03 ± 0.03 | 12 | 0.12 ± 0.32 | 48 | 0.26 ± 0.37 | 12.6 ± 14.1 | 4.88 ± 3.20 |
| Removal (%) | 97 | | 81 | | 81 | | 93 | | |

[1] % of (DRP + DUP + PP).

[2] Dissolved unreactive P (DUP) was calculated as the difference between total dissolved P and dissolved reactive P (DRP) while particulate P (PP) was calculated as the difference between total P (TP) and total dissolved P.
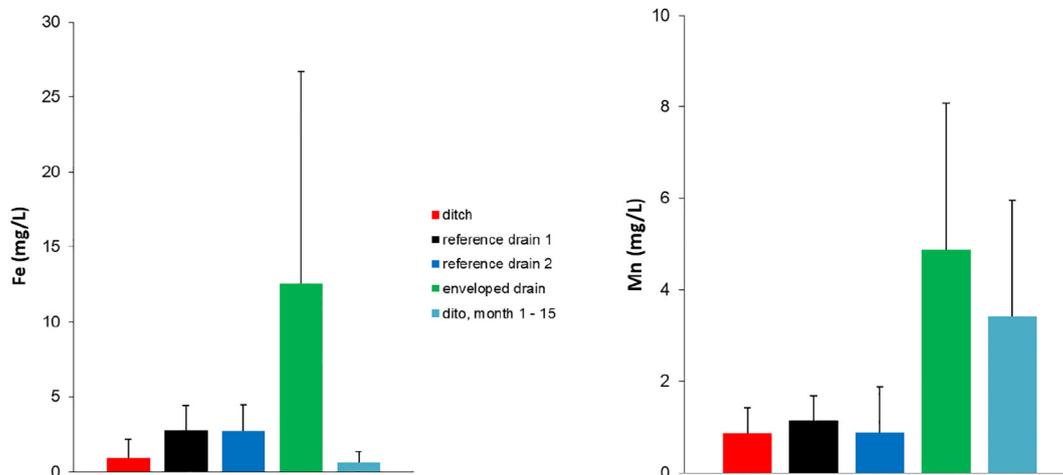
[3] Average of the two reference pipe drains.

**Fig. 3.** Total dissolved Fe (left) and Mn (right) concentrations in 0.45 μm-filtered water samples from the receiving ditch, the reference pipe drains and the enveloped pipe drain. Values represent average ± standard deviation over 54 months of the whole field experiment (n = 32). For total dissolved Fe and Mn concentrations from the enveloped pipe drain, the average values for the first 15 months are shown as well (Groenenberg et al., 2013). Please note difference in scale of y-axis of both figures.

concentration in the soil pore water from the subsoil with drainage water transported downward from above could explain why the average Fe concentrations in the effluents from the two reference pipe drains were so much lower. Indeed, the pore water sampled from the cups placed directly above the enveloped drain had an average Fe concentration of 1.2 mg Fe $L^{-1}$ (Table 1). When using the contributions of the downward drainage and upward seepage fluxes to the water influx into the pipe drains as calculated from the data on Cl (see Section 3.1.), the average Fe concentration in the effluents of the two reference pipe drains would be circa 13 mg $L^{-1}$, which is still much higher than the measured average Fe concentrations of circa 3 mg $L^{-1}$ (Fig. 3). Hence, oxidation of $Fe^{2+}$ and subsequent precipitation around or in the pipe drain must have contributed to the much lower Fe concentration leaching from the reference pipe drains.

Groenenberg et al. (2013) attributed the much lower Fe concentration in the effluent of the enveloped pipe drain during the first 15 months of the field experiment (Fig. 3) to retardation of $Fe^{2+}$ by adsorption onto Fh, or to an interaction between Fe(II) dissolved in the seepage water and Mn oxides, present in solid form in the Fe-coated sand used



**Fig. 4.** Total dissolved Fe and Mn concentrations in 0.45 μm-filtered water samples from the enveloped pipe drain as a function of time (32 sampling events over 54 months of the whole field experiment).

(3.1 mg $kg^{-1}$; Groenenberg et al., 2013), according to the reactions (Postma and Appelo, 2000):

$$2Fe^{2+} + MnO_2 + H_2O \leftrightarrow 2FeOOH + Mn^{2+} + 2H^+ \quad (1)$$

$$Fe^{2+} + MnOOH \leftrightarrow FeOOH + Mn^{2+} \quad (2)$$

Alternatively, the mineral Jacobsite ($MnFe_2O_4$) can be formed in a system where both $Fe^{2+}$ and $MnO_2$ are present, according to the reaction (Villinski et al., 2001, 2003):

$$2Fe^{2+} + MnO_2 + 2H_2O \leftrightarrow MnFe_2O_4 + 4H^+ \quad (3)$$
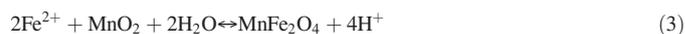
According to reaction (1), dissolved Fe(II) from the seepage water is oxidized in the envelope with Fe-coated sand to insoluble Fe(III) while insoluble Mn(IV) is reduced to dissolved Mn(II), with two moles of Fe being precipitated by reductive dissolution of one mole of Mn and with the production of two moles of $H^+$. According to reaction (2), insoluble Mn(III) is reduced to dissolved Mn(II), with one mole of Fe being precipitated by one mole of Mn and with no $H^+$ being produced. Indeed, the Mn concentration in the effluent of the enveloped pipe drain increased during the first circa 26 months of the field experiment, but then declined quite sharply (Fig. 4). Even more so, this decrease of the Mn concentration coincides with an increase in the Fe concentration in the enveloped pipe drain effluent (Fig. 4). However, the decrease of Mn in the drainage water cannot be explained by the exhaustion of the stock of Mn oxides supplied with the Fe-coated sand. Based on the amount of Mn in the Fe-coated sand around the pipe drain, the amount of water passing the drain, and the Mn concentration in the passing water, less than 8% of the initial Mn stock was leached during the whole experimental period of 54 months (see Section S1 in the Supplementary data). However, it is possible that the remaining Mn oxides react more slowly. A potential mechanism behind this could be that the readily accessible Mn oxide pool present on the outer surface of the Fe-coated sand was exhausted over time, or became covered by freshly precipitated Fe oxides (Villinski et al., 2003). Passivated Mn oxides or Mn oxides further inside the Fe coatings may react less readily with Fe(II) in the seepage water. Consequently, the Fe concentration in the effluent of the enveloped pipe drain increased gradually over time, either due to reductive dissolution of Fe oxides from the Fe-coated sand, or to breakthrough of $Fe^{2+}$ from the anoxic groundwater. Still, this did not lead to a concomitant release of DRP to the enveloped pipe drain effluent (Fig. 1). A comparable calculation for Fe as for Mn gave a value of <1% of the total amount of Fe initially present around the enveloped pipe drain
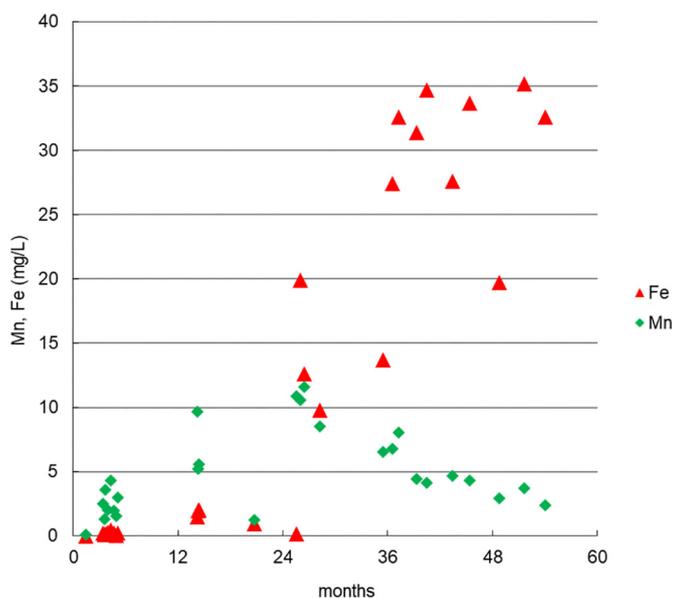
**Table 3**

Redox potential (Eh), pH, and chemical composition of the pore water measured within the SOFIE® cell at different layers of an undisturbed Fe-coated sand core taken from the enveloped pipe drain. The Fe-coated sand core was collected after 32 months ($t_{32}$).

| Layer | Depth | Eh | pH | Fe | Mn | $SO_4$-S | $NH_4$-N | $NO_3$-N | DRP | TDP |
|---|---|---|---|---|---|---|---|---|---|---|
| | cm | mV | | mg $L^{-1}$ | | | | | | |
| U[1] | 0.5 | −107 | 7.9 | 5.6 | 1.9 | 45 | 0.5 | 0.23 | <0.01 | 0.61 |
| M[1] | 5 | −219 | n.d.[2] | 9.4 | 3.4 | 36 | 4.5 | <0.02 | <0.01 | <0.01 |
| L[1] | 10 | −233 | 7.9 | 15.8 | 6.1 | 21 | 7.4 | <0.02 | <0.01 | <0.01 |

[1] Measurements were done in pore water collected from PES probes installed at several heights in the sediment core: one probe was installed just under the surface of the Fe-coated sand, denoted as the upper layer (U), another in the middle of the column, denoted as the middle layer (M), and the third one near the bottom, denoted as the lower layer (L).

that was leached during the whole experimental period (see Section S1 in the Supplementary data). In other words, an excess of Fe relative to adsorbed P is still present in the envelope with Fe-coated sand, explaining why the DRP concentration in the enveloped pipe drain effluent remained at a very low level over the entire period of the field experiment. This will be further discussed in Section 3.5.

### 3.4. Fe-coated sand: 0.01 M CaCl₂ extraction and SOFIE® cell

The concentrations of both DRP and TDP in the 0.01 $M$ CaCl₂ extracts of the Fe-coated sand from the different layers at $t_{32}$ and $t_{59}$ are all very low, as they are all below the detection limit (see Section S4 in the Supplementary data). Also, the levels of heavy metals and arsenic are very low in these extracts. However, these Fe-coated sand samples may have been exposed to oxic conditions during in-situ field sampling and subsequent freeze-drying and during the extraction with 0.01 $M$ CaCl₂, which may have influenced the analytical results. Therefore, an undisturbed Fe-coated sand core was sampled using the SOFIE® cell, which gave the opportunity to sample the pore water of the Fe-coated sand in the laboratory at redox-discrete field conditions. Table 3 gives a selection of the data measured using the SOFIE® cell while the complete data set is given in Table S2 in Section S2 in the Supplementary data. With increasing depth of the Fe-coated sand layer, the environment is more reduced as follows from the measured Eh. Based on the measured range in Eh, redox reactions including denitrification and reduction of Mn(III/IV) to Mn(II), Fe(III) to Fe(II), and $SO_4^{2-}$ to $S^{2-}$ could have occurred inside the envelope with Fe-coated sand (Pan et al., 2015). The gradient in Eh corresponds to the differences in the chemical composition of the pore water over the upper, middle, and lower Fe-coated sand layers (Table 3). Nitrate-N was only found in the upper layer; its concentration was below the detection limit in the middle and lower layers, which is probably due to denitrification. The concentrations of $NH_4$-N, Fe, and Mn increase with depth and the $SO_4$-S concentration decreased with depth (Table 3), corresponding with the trends seen for the suction cups (Table 1). The decrease with depth of the

$SO_4$-S concentration is probably due to sulfate reduction resulting from organic matter mineralization. The concentrations of DRP and TDP are below the detection limit in all layers. So no transfer of P through the Fe-coated sand envelope was observed, which is consistent with the very low levels of DRP leaching from the enveloped pipe drain over the whole field experiment (Fig. 1).

### 3.5. Composition of the Fe-coated sand

In Table 4, the total contents of Fe, Mn, and P as determined by digesting Fe-coated sand with Aqua Regia are summarized for $t_0$, $t_{14}$, $t_{32}$, and $t_{59}$. Data for Al are not presented as the Al contents in the Fe-coated sand were very small when compared to the Fe contents (< 1 mg $kg^{-1}$; data not shown). Based on the ratio of the total Fe content in the Fe-coated sand at $t_{59}$ relative to $t_0$, a large amount of Fe seems to have been lost from the envelope with Fe-coated sand over time, especially from the upper layer. The Fe fraction lost at $t_{59}$ amounted to 41, 25, and 27% for the upper, middle, and lower layers, respectively. However, leaching as an explanation would not be consistent with the calculated fraction of Fe leached as 0.3% of the initial total Fe content (see Section 3.3. and Section S1 in the Supplementary data). In addition to the Fe content, the total Mn and P contents decreased as well from $t_0$ to $t_{59}$. The apparent decrease in the contents of these elements could be due to a heterogeneous composition of the Fe-coated sand. The effect of the latter could have become particularly evident because Fe-coated sand samples were collected at different places along the enveloped pipe drain. However, this explanation seems unlikely as the total Fe, Mn, and P contents decrease over time in a consistent manner. Alternatively, the coating of the sand particles could have come off, either when the Fe-coated sand was applied during the installation of the enveloped pipe drain or during in-situ sampling in the field. The effect of loosening of the coating during Fe-coated sand application could especially explain the large decrease in the Fe content in the first 14 months of the field experiment (circa 20%). This large decrease in the Fe content cannot be explained by leaching of Fe. During these first 14 months, the Fe concentration in the enveloped pipe drain effluent was still low (Fig. 4), translating into a fraction of Fe leached over this period of only 0.003% of the total amount of Fe initially present around the enveloped pipe drain (see Section S1 in the Supplementary data). These Fe contents measured in the Fe-coated sand thus seem unreliable and cannot be used to calculate a mass balance of Fe in the envelope around the pipe drain. For this purpose, the loss of Fe from the envelope could be calculated from measurements of Fe in the pipe drain effluent in combination with an estimated effluent flux. Although this seems to be a more reliable approach because the effluent composition was measured at a large number of sampling events, which is the result of Fe release over the total length of the pipe drain, still the estimated effluent flux is uncertain. Unfortunately, Fe concentrations of Fe in the pipe drain effluent were only measured in 0.45 μm-filtered water samples. This could result in underestimating the loss of Fe from the enveloped pipe drain.

Due to the binding of P by the Fe-coated sand of the enveloped pipe drain over time, one would expect a gradual increase of the molar P/Fe

**Table 4**

Composition of Fe-coated sand measured using Aqua Regia digestion. The Fe-coated sand samples were taken after 0, 14, 32, and 59 months (denoted as $t_0$, $t_{14}$, $t_{32}$, and $t_{59}$).

| Sampling | Fe | | | Mn | | | P | | | P/Fe | | |
|---|---|---|---|---|---|---|---|---|---|---|---|---|
| | U[1] | M[1] | L[1] | U | M | L | U | M | L | U | M | L |
| | g $kg^{-1}$ | | | g $kg^{-1}$ | | | g $kg^{-1}$ | | | mol/mol | | |
| $t_0$[2] | 249 | 249 | 249 | 3.33 | 3.33 | 3.33 | 4.09 | 4.09 | 4.09 | 0.030 | 0.030 | 0.030 |
| $t_{14}$ | 200 | 200 | 195 | 2.59 | 2.55 | 1.96 | 3.55 | 3.48 | 3.01 | 0.032 | 0.031 | 0.028 |
| $t_{32}$ | 195 | 189 | 168 | 2.10 | 1.86 | 1.49 | 3.55 | 3.48 | 3.01 | 0.033 | 0.033 | 0.032 |
| $t_{59}$ | 148 | 187 | 181 | 1.76 | 1.83 | 1.82 | 2.75 | 3.26 | 3.43 | 0.033 | 0.031 | 0.034 |
| $t_{59}/t_0$ | 0.59 | 0.75 | 0.73 | 0.53 | 0.55 | 0.55 | 0.67 | 0.59 | 0.75 | | | |

[1] Samples were taken from three different layers of the Fe-coated sand envelope wrapped around the pipe drain where U denotes the upper layer, M the middle layer, and L the lower layer.

[2] For $t_0$, the composition of the Fe-coated sand for the three different layers is the same.

ratio in the coated sand. Indeed, this ratio showed a small increase from 0.030 at $t_0$ to 0.033 mol/mol (s.d. 0.0014) at $t_{59}$ when averaged over the three layers (Table 4). At this low molar P/Fe ratio, a strong adsorbing action of the Fe-coated sand is expected, even under reduced conditions (Young and Ross, 2001; Loeb et al., 2008). This explains the very low concentrations of DRP measured in the pore water in the SOFIE® cell (Table 3) and the very low DRP concentrations in the enveloped pipe drain effluent during the whole field experiment (Fig. 1). Using the measured TDP concentrations in the effluents of the pipe drains and estimated water fluxes, we calculated in Section S5 in the Supplementary data the retention of P by the enveloped pipe drain during the whole experimental period, and the resulting increase of the molar P/Fe ratio of the Fe-coated sand. For $t_{59}$, an increase to 0.031 mol/mol was calculated, which is close to the average P/Fe ratio of 0.033 mol/mol (s.d. 0.0014) found in the field. Based on the estimated P retention by the Fe-coated sand material, the annual reduction in P loss by enveloping pipe drains with Fe-coated sand at the field scale can be extrapolated to 19 kg P ha$^{-1}$ (see Section S5 in the Supplementary data).

Results from the characterization of Fe-coated sand sampled at $t_0$ and $t_{32}$ by Fe K-edge EXAFS spectroscopy are shown in Fig. S2 in Section S6 in the Supplementary data. The marked oscillations in the k-space EXAFS spectra of lepidocrocite and goethite (Fig. S2a) arise from the edge-sharing (Lp and Goe) and corner-sharing (Goe) coordination of FeO$_6$-octahedra, as can be seen in the corresponding Fourier-transformed spectra (Fig. S2b). The spectra of the two nanocrystalline Fh references (2L-Fh and Si-Fh) feature much lower second-shell FeFe signal amplitudes, due to a lower degree and less-ordered second-shell FeFe coordination. The minor differences between the two Fh references arise from a lower distortion of the FeO$_6$ octahedra and a lower degree of corner-sharing FeFe linkage in silicate-ferrihydrite (Si-Fh) than 2-line ferrihydrite (2L-Fh), reflecting a lower degree of Fe polymerization in Si-Fh formed by Fe(II) oxidation in bicarbonate-buffered solution in the presence of silicate than 2L-Fh formed by base addition to an acidic Fe (III) solution. The spectrum of the Fe-coated sand sampled at $t_0$ falls in between the spectra of Si-Fh and 2L-Fh, and can be adequately reproduced by a linear combination of the two Fh reference spectra (0.78 Si-Fh + 0.20 2L-Fh). The Fe-coatings of the sand particles were formed during water treatment by the oxidation of Fe(II) in oxygenated groundwater in the presence of silicate (Chardon et al., 2012; Koopmans et al., 2020), in analogy to the synthesis of the Si-Fh reference. The slightly higher degree of Fe polymerization in the coatings than the Si-Fh reference material may indicate that the coatings were either formed at a slightly lower dissolved Si/Fe ratio than the Si-Fh reference or that siliceous Fh in the coatings of sand sampled at $t_0$ had already aged and further polymerized compared to freshly precipitated Si-Fh. The latter explanation is probable, as sand can be used over several years in filters used for water treatment in drinking water production plants before replacement (Sharma et al., 2002), allowing the Fe(III) precipitates to age in contact with aerated Fe(II)-containing water over an extended period of time. Comparison of the spectra of the 32-months field-aged Fe-coated sand from the three different layers and the spectrum of the Fe-coated sand at $t_0$ indicated no marked changes in Fe coordination over 32 months, irrespective of the sampled layer. Considering the intense signal amplitudes of the goethite and lepidocrocite reference spectra (Fig. S2), this indicates that at most a very small fraction of the ferrihydrite had transformed into goethite or lepidocrocite within 32 months. However, because the anoxic state of the Fe-coated sand sample from the lower layer could not be maintained during sample preparation and analysis in the laboratory, some Fe(II) associated with this sample, either as Fe$^{2+}$ adsorbed onto Fh or as a mixed valence Fe(II/III) phase, may have been overlooked in the fit. Nevertheless, these Fe(II)-phases probably did not account for a major fraction of the total Fe because there is a close match between the three spectra from the three different layers.

The initial Fe-coated sand sampled at $t_0$ and the Fe-coated sand samples aged in-situ for 32 months ($t_{32}$) in the field were further characterized by an acid ammonium oxalate extraction aimed at dissolving amorphous or poorly crystalline Fe oxides like Fh (Schwertmann, 1991). Table S6 in

Section S6 in the Supplementary data presents data on Fe$_{ox}$, Mn$_{ox}$, and P$_{ox}$ in the Fe-coated sand sampled at $t_{32}$ and $t_{59}$. The extracted amounts of Al$_{ox}$ in these samples were negligible (data not shown). The same was found for iron oxide sludge, produced as a byproduct at the same drinking water production plant (Koopmans et al., 2020). At $t_{32}$, the measured Fe$_{ox}$, Mn$_{ox}$, and P$_{ox}$ contents of the upper and middle layers are only slightly lower than the contents determined by Aqua Regia digestion. For Fe, this is qualitatively in line with the characterization of the solid phase Fe as Fh by EXAFS, as discussed above. For the lower layer, however, the Fe$_{ox}$, Mn$_{ox}$, and P$_{ox}$ contents at $t_{32}$ are clearly lower than for Aqua Regia. Likewise, the Fe$_{ox}$, Mn$_{ox}$, and P$_{ox}$ contents in the samples from all three layers at $t_{59}$ are much lower than the contents determined by Aqua Regia digestion. Since the EXAFS spectrum of the sample from the lower layer taken at $t_{32}$ was similar to the two spectra from the upper and middle layers (Fig. S2), the discrepancy between the Fe$_{ox}$ content and the Fe content determined by Aqua Regia digestion cannot be explained by substantial Fh transformation into more crystalline compounds. Unfortunately, no EXAFS data are available for the samples collected at $t_{59}$ to validate this observation. Rather than transformation of Fh into more crystalline compounds, the effect of loosening of the Fe-coating of the sand particles when taking subsamples from the Fe-coated sand samples in the laboratory for the acid ammonium oxalate extraction and Aqua Regia digestion may explain the discrepancy between the contents of Fe, Mn, and P as determined by the two methods. For the Aqua Regia digestion, ground Fe-coated sand (50 μm) was used (Houba et al., 1997), whereas unground material was used for the acid ammonium oxalate extraction. Since the Fe-coated sand samples may have been non-homogeneous due to the loose Fe oxide coating of the sand particles, it may have been difficult to obtain a representative subsample, causing an underestimation of the Fe$_{ox}$, Mn$_{ox}$, and P$_{ox}$ contents if the subsample contained mainly coarse sand particles (Neary and Barnes, 1993). Based on the results of the characterization of Fe-coated sand samples by Fe K-edge EXAFS and the very low DRP concentrations from the enveloped pipe drain over the whole field experiment, the submerged conditions of the enveloped pipe drain did not seem to affect the stability of Fh in the Fe-coated sand and its ability to capture P from drainage water.

## 4. Conclusions

- Enveloping a pipe drain with Fe-coated sand resulted in an average DRP removal of 93%, over a period of 4.5 years. No indication was found of a decrease in effectiveness with time. The enveloped pipe drain resulted in effluent concentrations that were below the Dutch water quality criterion of 0.15 mg TP L$^{-1}$.
  - While during the first 2 years of the experiment Mn oxides present in the Fe-coated sand prevented the reductive release of Fe(II) and P from Fe(III) oxides in the Fe-coated sand, this effect was not found during the latter part of the experiment. This is possibly due to a depletion of easily accessible Mn oxides.
  - The loss of Fe, calculated from the concentrations of Fe in the effluent from the enveloped pipe drain, was insignificant when compared to the amount of Fe around the drain.
  - No indications were found for a structural change of the Fe-coatings over the course of the field experiment. Using Fe K-edge EXAFS spectroscopy, it was concluded that the Fe in the coating of the sand particles was mainly present as silicate-containing Fh.

## Declaration of competing interest

## Acknowledgments

## Appendix A. Supplementary data

Supplementary data to this article can be found online at https://doi.org/10.1016/j.scitotenv.2021.152738.

## References

Baken, S., Nawara, S., van Moorleghem, C., Smolders, E., 2014. Iron colloids reduce the bioavailability of phosphorus to the green alga Raphidocelis subcapitata. Water Res. 59, 198–206. https://doi.org/10.1016/j.watres.2014.04.010.

Baken, S., Verbeeck, M., Verheyen, D., Diels, J., Smolders, E., 2015. Phosphorus losses from agricultural land to natural waters are reduced by immobilization in iron-rich sediments of drainage ditches. Water Res. 71, 160–170. https://doi.org/10.1016/j.watres.2015.01.008.

van Beek, C.G.E.M., 2018. Well-screen and well-head clogging by hydrous ferric oxides. Hydrogeol. J. 26, 2919–2932. https://doi.org/10.1007/s10040-018-1822-2.

Buda, A.R., Koopmans, G.F., Bryant, R.B., Chardon, W.J., 2012. Emerging technologies for removing nonpoint phosphorus from surface water and groundwater: introduction. J. Environ. Qual. 41, 621–627. https://doi.org/10.2134/jeq2012.0080.

Canga, E., Heckrath, G., Kjaergaard, C., 2016a. Agricultural drainage filters. II. Phosphorus retention and release at different flow rates. Water Air Soil Pollut. 227, 276. https://doi.org/10.1007/s11270-016-2963-3.

Canga, E., Kjaergaard, C., Iversen, B.V., Heckrath, G., 2016b. Agricultural drainage filters. I. Filter hydro-physical properties and tracer transport. Water Air Soil Pollut. 227, 289. https://doi.org/10.1007/s11270-016-2987-8.

Celi, L., De Luca, G., Barberis, E., 2003. Effects of interaction of organic and inorganic P with ferrihydrite and kaolinite-iron oxide systems on iron release. Soil Sci. 168, 479–488. https://doi.org/10.1097/01.ss.0000080333.10341.a4.

Chardon, W.J., Schoumans, O.F., 2007. Soil texture effects on the transport of phosphorus from agricultural land in river deltas of Northern Belgium, The Netherlands and North-West Germany. Soil Use Manag. 23 (Suppl. 1), 16–24. https://doi.org/10.1111/j.1475-2743.2007.00108.x.

Chardon, W.J., Groenenberg, J.E., Temminghoff, E.J.M., Koopmans, G.F., 2012. Use of reactive materials to bind phosphorus. J. Environ. Qual. 41, 636–646. https://doi.org/10.2134/jeq2011.0055.

Cucarella, V., Renman, G., 2009. Phosphorus sorption capacity of filter materials used for on-site wastewater treatment determined in batch experiments-a comparative study. J. Environ. Qual. 38, 381–392.

Griffioen, J., 1994. Uptake of phosphate by iron hydroxides during seepage in relation to development of groundwater composition in coastal areas. Environ. Sci. Technol. 28, 675–681. https://doi.org/10.1021/es00053a022.

Groenenberg, J.E., Chardon, W.J., Koopmans, G.F., 2013. Reducing phosphorus loading of surface water using iron-coated sand. J. Environ. Qual. 42, 250–259. https://doi.org/10.2134/jeq2012.0344.

Haygarth, P.M., Sharpley, A.N., 2000. Terminology for phosphorus transfer. J. Environ. Qual. 29, 10–15.

Hiemstra, T., 2018. Ferrihydrite interaction with silicate and competing oxyanions: geometry and hydrogen bonding of surface species. Geochim. Cosmochim. Acta 238, 453–476. https://doi.org/10.1016/j.gca.2018.07.017.

Hiemstra, T., van Riemsdijk, W.H., 1996. A surface structural approach to ion adsorption: the charge distribution (CD) model. J. Colloid Interface Sci. 179, 488–508. https://doi.org/10.1006/jcis.1996.0242.

Hiemstra, T., Zhao, W., 2016. Reactivity of ferrihydrite and ferritin in relation to surface structure, size, and nanoparticle formation studied for phosphate and arsenate. Environ. Sci. Nano 3, 1265–1279. https://doi.org/10.1039/c6en00061d.

Hiemstra, T., Mendez, J.C., Li, J., 2019. Evolution of the reactive surface area of ferrihydrite: time, pH, and temperature dependency of growth by Ostwald ripening. Environ. Sci. Nano 6, 820–833. https://doi.org/10.1039/c8en01198b.

Houba, V.J.G., van der Lee, J.J.G., Novozamsky, I., 1997. Soil and Plant Analysis. Part 1: Soil Analysis Procedures. Wageningen University, Wageningen, The Netherlands.

Houba, V.J.G., Temminghoff, E.J.M., Gaikhorst, G.A., van Vark, W., 2000. Soil analysis procedures using 0.01 M calcium chloride as extraction reagent. Commun. Soil Sci. Plant Anal. 31, 1299–1396. https://doi.org/10.1080/00103620009370514.

Kaegi, R., Voegelin, A., Folini, D., Hug, S.J., 2010. Effect of phosphate, silicate, and Ca on the morphology, structure and elemental composition of Fe(III)-precipitates formed in aerated Fe(II) and As(III) containing water. Geochim. Cosmochim. Acta 74, 5798–5816. https://doi.org/10.1016/j.gca.2010.07.017.

King, K.W., Williams, M.R., Macrae, M.L., Fausey, N.R., Frankenberger, J., Smith, D.R., Kleinman, P.J.A., Brown, L.C., 2015. Phosphorus transport in agricultural subsurface drainage: a review. J. Environ. Qual. 44, 467–485.

Kirk, G., 2004. The Biogeochemistry of Submerged Soils. John Wiley & Sons Ltd, Chichester, England.

Kleinman, P.J.A., 2017. The persistent environmental relevance of soil phosphorus sorption saturation. Curr. Pollut. Rep. 3, 141–150.

Kleinman, P.J.A., Sharpley, A.N., Buda, A.R., McDowell, R.W., Allen, A.L., 2011. Soil controls of phosphorus in runoff: management barriers and opportunities. Can. J. Soil Sci. 91, 329–338.

Klimeski, A., Chardon, W.J., Uusitalo, R., Turtola, E., 2012. Potential and limitations of phosphate retention media in water protection: a process-based review of laboratory and field-scale tests. Agric. Food Sci. 21, 206–223.

Koopmans, G.F., Chardon, W.J., Ehlert, P.A.I., Dolfing, J., Suurs, R.A.A., Oenema, O., van Riemsdijk, W.H., 2004. Phosphorus availability for plant uptake in a phosphorus-enriched noncalcareous sandy soil. J. Environ. Qual. 33, 965–975. https://doi.org/10.2134/jeq2004.0965.

Koopmans, G.F., Chardon, W.J., Dekker, P.H.M., Römkens, P.F.A.M., Schoumans, O.F., 2006. Comparing different extraction methods for estimating phosphorus solubility in various soil types. Soil Sci. 171, 103–116.

Koopmans, G.F., Hiemstra, T., Vaseur, C., Chardon, W.J., Voegelin, A., Groenenberg, J.E., 2020. Use of iron oxide nanoparticles for immobilizing phosphorus in-situ: increase in soil reactive surface area and effect on soluble phosphorus. Sci. Total Environ. 711. https://doi.org/10.1016/j.scitotenv.2019.135220.

Loeb, R., Lamers, L.P.M., Roelofs, J.G.M., 2008. Prediction of phosphorus mobilisation in inundated floodplain soils. Environ. Pollut. 156, 325–331.

Macintosh, K.A., Mayer, B.K., McDowell, R.W., Powers, S.M., Baker, L.A., Boyer, T.H., Rittmann, B.E., 2018. Managing diffuse phosphorus at the source versus at the sink. Environ. Sci. Technol. 52, 11995–12009. https://doi.org/10.1021/acs.est.8b01143.

McCrackin, M.L., Muller-Karulis, B., Gustafsson, B.G., Howarth, R.W., Humborg, C., Svanback, A., Swaney, D.P., 2018. A century of legacy phosphorus dynamics in a large drainage basin. Glob. Biogeochem. Cycles 32, 1107–1122. https://doi.org/10.1029/2018GB005914.

McDowell, R.W., Sharpley, A.N., Bourke, W., 2008. Treatment of drainage water with industrial by-products to prevent phosphorus loss from tile drained land. J. Environ. Qual. 37, 1575–1582. https://doi.org/10.2134/jeq2007.0454.

McKeague, J.A., Day, J.H., 1966. Dithionite and oxalate-extractable Fe and Al as aids in differentiating various classes of soils. Can. J. Soil Sci. 46, 13–22.

Murphy, J., Riley, J.P., 1962. A modified single solution method for the determination of phosphate in natural waters. Anal. Chim. Acta 27, 31–36. https://doi.org/10.1016/S0003-2670(00)88444-5.

Neary, A.J., Barnes, S.R., 1993. The effect of sample grinding on extractable iron and aluminum in soils. Can. J. Soil Sci. 73, 73–80.

Nielsen, S.S., Kjeldsen, P., Hansen, H.C.B., Jakobsen, R., 2014. Transformation of natural ferrihydrite aged in situ in As, Cr and Cu contaminated soil studied by reduction kinetics. Appl. Geochem. 51, 293–302.

Pan, Y.Y., Koopmans, G.F., Bonten, L.T.C., Song, J., Luo, Y.M., Temminghoff, E.J.M., Comans, R.N.J., 2015. In-situ measurement of free trace metal concentrations in a flooded paddy soil using the Donnan Membrane Technique. Geoderma 241–242, 59–67. https://doi.org/10.1016/j.geoderma.2014.11.003.

Penn, C., McGrath, J., Bowen, J., Wilson, S., 2014. Phosphorus removal structures: a management option for legacy phosphorus. J. Soil Water Conserv. 69, 51A–56A. https://doi.org/10.2489/jswc.69.2.51A.

Penn, C., Chagas, I., Klimeski, A., Lyngsie, G., 2017. A review of phosphorus removal structures: how to assess and compare their performance. Water 9, 583. https://doi.org/10.3390/w9080583.

Postma, D., Appelo, C.A.J., 2000. Reduction of Mn-oxides by ferrous iron in a flow system: column experiment and reactive transport modeling. Geochim. Cosmochim. Acta 64, 1237–1247. https://doi.org/10.1016/S0016-7037(99)00356-7.

Quevauviller, P., 1998. Operationally defined extraction procedures for soil and sediment analysis I.Standardization. Trends Anal. Chem. 17, 289–298.

Ravel, B., Newville, M., 2005. ATHENA, ARTEMIS, HEPHAESTUS: data analysis for X-ray absorption spectroscopy using IFEFFIT. J. Synchrotron Radiat. 12, 537–541.

van der Salm, C., Chardon, W.J., Koopmans, G.F., van Middelkoop, J.C., Ehlert, P.A.I., 2009. Phytoextraction of phosphorus-enriched grassland soils. J. Environ. Qual. 38, 751–761. https://doi.org/10.2134/jeq2008.0068.

Schoumans, O.F., 2000. Determination of the degree of phosphate saturation in noncalcareous soils. In: Pierzynski, G.M. (Ed.), Methods of Phosphorus Analysis for Soils, Sediments, Residuals, and Waters. Southern Coop. Ser. Bull396, pp. 31–34 USA.

Schoumans, O.F., 2014. Description of the phosphorus sorption and desorption processes in coarse calcareous sandy soils. Soil Sci. 179, 221–229 doi:0.1097/SS.0000000000000065.

Schoumans, O.F., Chardon, W.J., 2015. Phosphate saturation degree and accumulation of phosphate in various soil types in the Netherlands. Geoderma 237–238, 325–335. https://doi.org/10.1016/j.geoderma.2014.08.015.

Schwertmann, U., 1964. Differenzierung der Eisenoxide des Bodens durch Extraktion mit Ammoniumoxalat-Lösung. Z. Pflanzenernähr. Düng. Bodenk. 105, 194–202. https://doi.org/10.1002/jpln.3591050303.

Schwertmann, U., 1991. Solubility and dissolution of iron oxides. Plant Soil 130, 1–25.

Schwertmann, U., Cornell, R.M., 1991. Iron Oxides in the Laboratory. VCH, Weinheim, Germany.

Senn, A.C., Kaegi, R., Hug, S.J., Hering, J.G., Mangold, S., Voegelin, A., 2015. Composition and structure of Fe(III)-precipitates formed by Fe(II) oxidation in near-neutral water: interdependent effects of phosphate, silicate and ca. Geochim. Cosmochim. Acta 162, 220–246. https://doi.org/10.1016/j.gca.2015.04.032.

Sharma, S.K., Petrusevski, B., Schippers, J.C., 2002. Characterisation of coated sand from iron removal plants. Water Sci. Technol. Water Supply Lond. 2 (2), 247–257.

Sharpley, A.N., Jarvie, H.P., Buda, A., May, L., Spears, B., Kleinman, P., 2013. Phosphorus legacy: overcoming the effects of past management practices to mitigate future water quality impairment. J. Environ. Qual. 42, 1308–1326.

Stroom, J.M., Kardinaal, W.E.A., 2016. How to combat cyanobacterial blooms: strategy toward preventive lake restoration and reactive control measures. Aquat. Ecol. 50, 541–576.

Vandermoere, S., Ralaizafisoloarivony, N.A., van Ranst, E., De Neve, S.A.F., 2018. Reducing phosphorus (P) losses from drained agricultural fields with iron coated sand (- glauconite) filters. Water Res. 141, 329–339. https://doi.org/10.1016/j.watres.2018.05.022.

Villinski, J.E., O'Day, P.A., Corley, T.L., Conklin, M.H., 2001. In situ spectroscopic and solution analyses of the reductive dissolution of MnO2 by Fe(II). Environ. Sci. Technol. 35, 1157–1163. https://doi.org/10.1021/es001356d.

Villinski, J.E., Saiers, J.E., Conklin, M.H., 2003. The effects of reaction-product formation on the reductive dissolution of MnO2 by Fe(II). Environ. Sci. Technol. 37, 5589–5596. https://doi.org/10.1021/es034060r.

Vink, J.P.M., 2002. Measurement of heavy metal speciation over redox gradients in natural water-sediment interfaces and implications for uptake by benthic organisms. Environ. Sci. Technol. 36, 5130–5138. https://doi.org/10.1021/es0200701.

Vink, J.P.M., 2009. The origin of speciation: trace metal kinetics over natural water/sediment interfaces and the consequences for bioaccumulation. Environ. Pollut. 157, 519–527. https://doi.org/10.1016/j.envpol.2008.09.037.

Vink, J.P.M., Harmsen, J., Rijnaarts, H., 2010. Delayed immobilization of heavy metals in soils and sediments under reducing and anaerobic conditions. Consequences for flooding and storage. J. Soils Sedim. 10, 1633–1645.

Voegelin, A., Weber, F.A., Kretzschmar, R., 2007. Distribution and speciation of arsenic around roots in a contaminated riparian floodplain soil: micro-XRF element mapping and EXAFS spectroscopy. Geochim. Cosmochim. Acta 71, 5804–5820. https://doi.org/10.1016/j.gca.2007.05.030.

Voegelin, A., Kaegi, R., Frommer, J., Vantelon, D., Hug, S.J., 2010. Effect of phosphate, silicate, and Ca on Fe(III)-precipitates formed in aerated Fe(II)- and As(III)- containing water studied by X-ray absorption spectroscopy. Geochim. Cosmochim. Acta 74, 164–186. https://doi.org/10.1016/j.gca.2009.09.020.

Wang, X., Li, W., Harrington, R., Liu, F., Parise, J.B., Feng, X., Sparks, D.L., 2013. Effect of ferrihydrite crystallite size on phosphate adsorption reactivity. Environ. Sci. Technol. 47, 10322–10331. https://doi.org/10.1021/es401301z.

Young, E.O., Ross, D.S., 2001. Phosphate release from seasonally flooded soils: a laboratory microcosm study. J. Environ. Qual. 30, 91–101.